Bioorganic & Medicinal Chemistry 17 (2009) 614–620

Contents lists available at ScienceDirect

Bioorganic & Medicinal Chemistry

journal homepage: www.elsevier.com/locate/bmc

DNA binding, cytotoxicity, apoptotic inducing activity, and molecular modeling study of quercetin zinc(II) complex

Jun Tan [a,b,c,*], Bochu Wang [a,*], Liancai Zhu [a]

[a] Bioengineering College, Chongqing University, Chongqing 400030, China
[b] Department of Life Science and Chemistry, Chongqing Education College, Chongqing 400067, China
[c] Post-doctoral Research Center of Mechanics, Mechanical Resource and Environment College, Chongqing University, Chongqing 400030, China

ARTICLE INFO

Article history:
Received 4 October 2008
Revised 23 November 2008
Accepted 25 November 2008
Available online 3 December 2008

Keywords:
Quercetin zinc(II) complex
DNA binding
Intercalation
Antitumor activity

ABSTRACT

DNA cleavage activity of quercetin zinc(II) complex has been studied, but little attention has been devoted to the relationship between antitumor activity of this complex and DNA-binding properties. DNA-binding properties of quercetin zinc(II) complex were studied using UV–vis spectra, fluorescence measurements, and viscosity measurements. The results obtained indicate that quercetin zinc(II) complex can intercalate into the stacked base pairs of DNA, and compete with the strong intercalator ethidium bromide for the intercalative binding sites with Stern–Volmer quenching constant, K_{sq} = 1.24. The complex was subjected to biological tests in vitro using three tumor cell lines (HepG2, SMMC7721, and A549), which showed significant cytotoxicity against three tumor cell lines. Moreover, Hoechst33258 staining showed HepG2 cells underwent the typical morphologic changes of apoptosis characterized by nuclear shrinkage, chromatin condensation, or fragmentation after exposure to the complex. In addition, Molecular modeling was performed to learn the complex could be preferentially bound to DNA in GC region. Our results suggest that antitumor activity of quercetin zinc(II) complex might be related to its intercalation into DNA.

© 2008 Elsevier Ltd. All rights reserved.

1. Introduction

In recent years, many researches[1–3] have been focused on interaction of small molecules with DNA. DNA is generally the primary intracellular target of anticancer drugs, so the interaction between small molecules and DNA can cause DNA damage in cancer cells, blocking the division of cancer cells, and resulting in cell death.[4,5] Small molecule can interact with DNA through the following three non-covalent modes: intercalation, groove binding, and external static electronic effects. Among these interactions, intercalation is one of the most important DNA-binding modes, which is related to the antitumor activity of the compound. Recently, there is a great interest on the binding of transition metal complexes with DNA, owing to their possible applications as new cancer therapeutic agents and their photochemical properties that make them potential probes of DNA structure and conformation.[6–8] Especially, binding of zinc(II) complexes to DNA has attracted much attention.[9,10] It has been reported that the intercalating ability of the complex was involved in the planarity of ligands, the coordination geometry, ligand donor atom type, the metal ion type.[11–13] So the development of synthetic, sequence-selective DNA binding and cleavage agents for DNA itself and for new potential DNA-targeted antitumor drugs is essential for further expected applications in molecular biology, medicine, and related fields.

Quercetin (Que, 3,5,7,3′,4′-pentahydroxyflavone), a bioflavonoid widely distributed in fruits and vegetables, has been reported to exert multiple biological effects as an antioxidant and antitumor activity.[14–17] Quercetin can chelate metal ions to form metal complexes that have better antioxidation and antitumor activity than quercetin alone.[18,19] In our previous work, we demonstrated that quercetin zinc(II) complex, $Zn(Que)_2(H_2O)_2$ (Fig. 1), can cleave the DNA via hydrolytic pathway.[20,21] However, little research has been devoted to the relationship between the better antitumor activity of quercetin zinc(II) complex and its DNA-binding properties.

In this study, we investigated the mode of DNA binding, cytotoxicity, apoptotic inducing activity of quercetin zinc(II) complex. We demonstrate quercetin zinc(II) complex could be preferentially bound to DNA in GC region via an intercalation mode, involved in antitumor activity of the complex.

2. Results and discussion

2.1. DNA-binding properties

The binding of quercetin zinc(II) complex with calf thymus DNA (CT DNA) was measured using absorption, fluorescence spectrophotometric titrations, and viscosity measurements.

* Corresponding authors. Address: Bioengineering College, Chongqing University, Chongqing 400030, China. Tel.: +86 23 62658256; fax: +86 23 62657812 (J. Tan).
E-mail addresses: tanjun1976@hotmail.com (J. Tan), wangbc2000@126.com (B. Wang).

0968-0896/$ - see front matter © 2008 Elsevier Ltd. All rights reserved.
doi:10.1016/j.bmc.2008.11.063

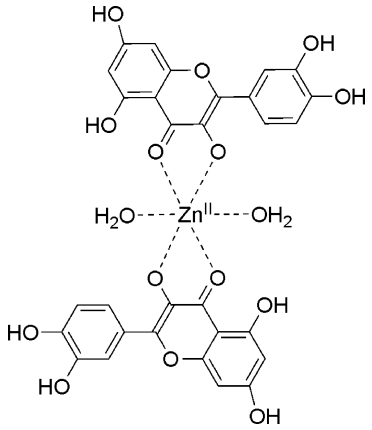

Figure 1. The tentative structure of quercetin zinc(II) complex.

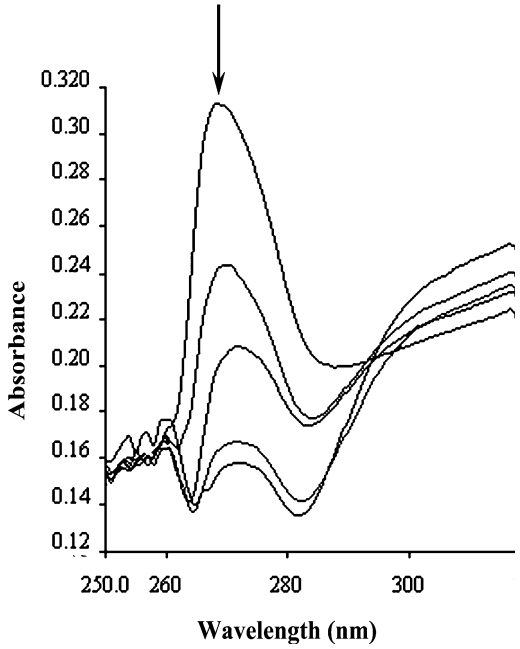

Figure 2. Absorption spectra of quercetin zinc(II) complex (10 μM) in 0.01 M Tris–HCl buffer at pH 7.2, in the absence and presence of increasing amounts of CT DNA (from top to bottom, 0–40 μM bp). The arrow shows the intensity decreased with increasing concentration of the complex.

The binding of the complex to DNA has been characterized classically through absorption titration. A complex bound to DNA through intercalation is characterized by the change in absorbance (hypochromism) and red-shift in wavelength, due to the intercalative mode involving a stacking interaction between the aromatic chromophore and the DNA base pairs. The electronic absorption spectra of $Zn(Que)_2(H_2O)_2$ complex exhibited broad absorption bands in the region 250–320 nm, typical for transitions between the π-electronic energy levels of the quercetin skeleton. The electronic spectra of the complex in the presence and absence of DNA were monitored at a wavelength range of 250–320 nm, as shown in Figure 2. Upon the increasing of concentration of CT DNA (0–40 μM), a considerable drop in the absorptivity (60% hypochromicity) at about 270 nm and a substantial red-shift ($\Delta\lambda$ = 6 nm) was observed. The hypochromicity suggests $Zn(Que)_2(H_2O)_2$ complex may bind to DNA by intercalation mode, due to a strong interaction between the electronic states of the intercalating chromophore and those of the DNA bases.

The additional evidence for intercalation into the DNA was obtained from fluorescence spectral studies. The fluorescence spectra of $Zn(Que)_2(H_2O)_2$ complex, exhibiting a broad emission band in the range 340–360 nm, were monitored at a fixed concentration of 30 μM. Enhanced fluorescence without wavelength shift was observed (Fig. 3), when CT DNA was added into the complex solution. The result suggests that the stronger enhancement of fluorescence intensity for the complex may be largely due to the interaction between adjacent base pairs of CT DNA and the complex. Furthermore, the binding of the complex to the DNA helix could decrease the collisional frequency solvent molecules with the complex, which usually leads to emission enhancement of the complex. The result also agrees with those observed for other intercalators.[1,7,8] So the complex may intercalate into the adjacent base pairs of CT DNA. In addition, Figure 4 shows the fluorescence intensity of the complex increased when the different kinds of DNA were added into the complex solution. In Figure 4, I_0 and I represent the fluorescence intensities in the absence or presence of the DNA, respectively. The result illustrates that there is the largest increase in fluorescence intensity as the poly(dG)·poly(dC) added into the complex solution. So the binding affinity between complex and the poly(dG)·poly(dC) may be larger than that between the complex and CT DNA (or the poly(dA)·poly(dT)).

To understand the interaction pattern of the complex with DNA more clearly, fluorometric competitive binding experiment was carried out using ethidium bromide (EB) as a probe that

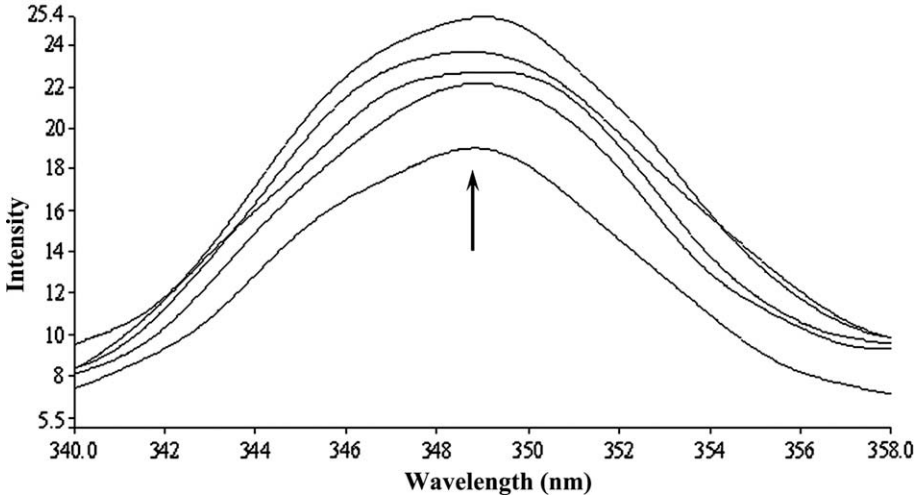

Figure 3. The change of emission fluorescence spectra of quercetin zinc(II) complex (30 μM) in 0.01 M Tris–HCl buffer at pH 7.2, in the absence and presence of increasing amounts of CT DNA (from bottom to top, 0–60 μM bp), λ_{ex} = 312 nm. The arrow shows the intensity increased with increasing concentration of the complex.

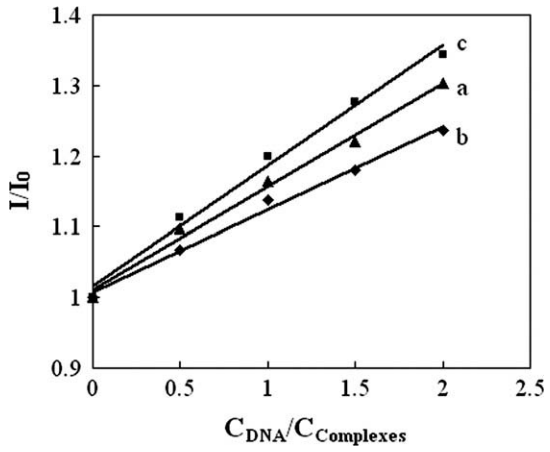

Figure 4. Effects of CT DNA (a), poly(dA)·poly(dT) (b), and poly(dG)·poly(dC) (c) on relative fluorescence intensity of quercetin zinc(II) complex. The CT DNA, poly(dA)·poly(dT), and poly(dG)·poly(dC) were added into the complex solution, respectively. Emission spectra were recorded in the region 330–370 nm using an excitation wavelength of 312 nm. I_0 and I represent the fluorescence intensities in the absence or presence of the complex, respectively.

shows no apparent emission intensity in buffer solution because of solvent quenching. However, EB emits intense fluorescent light in the presence of DNA due to its strong intercalation between the adjacent DNA base pairs. A competitive binding of small molecular to CT DNA could result in the displacement of EB or quenching of the bound EB by the compound decreasing its emission intensity. It was previously reported that the enhanced fluorescence could be quenched by the addition of another molecules.[1,13] The emission spectra of EB bound to DNA in the absence and in the presence of $Zn(Que)_2(H_2O)_2$ complex are given in Figure 5. The emission band at 587 nm of the DNA–EB system decreased in intensity with the increasing concentration of the complex, and an equal absorption point appeared at 543.2 nm (data not shown). It has been reported that small organic molecules interact with DNA by intercalation when the concentration ratio of them to DNA (c_M/c_{DNA}) is less than 100 and the fluorescence intensity of EB–DNA system decreases by 50%.[1,22] The inset in Figure 5 shows the quenching extent has reached up to 60% when $c_{complex}/c_{DNA}$ = 1.2. The changes observed here are often characteristic of intercalation. Moreover, this phenomenon indicates that $Zn(Que)_2(H_2O)_2$ complex competes with EB in binding to DNA.

According to the classical Stern–Volmer equation:[23]

$$\frac{I_0}{I} = 1 + K_{sq}r \quad (1)$$

where I_0 and I represent the fluorescence intensities in the absence or presence of the complex, respectively, and r is the concentration ratio of the complex to DNA. K_{sq} is a linear Stern–Volmer quenching constant dependent on the ratio of the bound concentration of EB to the concentration of DNA (Fig. 5, inset). The K_{sq} value is obtained as the slope of I_0/I versus r linear plot. From the inset in Figure 5, the K_{sq} value for $Zn(Que)_2(H_2O)_2$ complex is 1.24, which suggests that the interaction of the complex with DNA is strong.[24] It may be

Table 1
Effect of quercetin and quercetin zinc(II) complex on the viability[a] of tumor cells

Tumor cells	Time (h)	IC_{50} (μmol L^{-1})	
		$(Quecetin)_2$	$Zn(Que)_2(H_2O)_2$
HepG2	24	49.28 ± 1.25	20.04 ± 0.97
	48	33.69 ± 1.01	10.67 ± 0.83
	72	13.30 ± 0.96	5.46 ± 0.36
SMMC7721	24	63.11 ± 1.19	27.36 ± 0.89
	48	42.12 ± 1.03	14.10 ± 0.68
	72	27.53 ± 0.95	7.66 ± 0.30
A549	24	103.89 ± 1.44	51.63 ± 1.02
	48	72.12 ± 1.15	21.03 ± 0.88
	72	34.88 ± 1.06	10.00 ± 0.45

[a] Cell viabilities were evaluated by MTT assays. Cells were incubated for 0–72 h without (control) or with 0–100 μM of the tested compound. IC_{50} are concentrations which produced 50% inhibition of the cell viability. Results are expressed as means ± SD (n = 3).

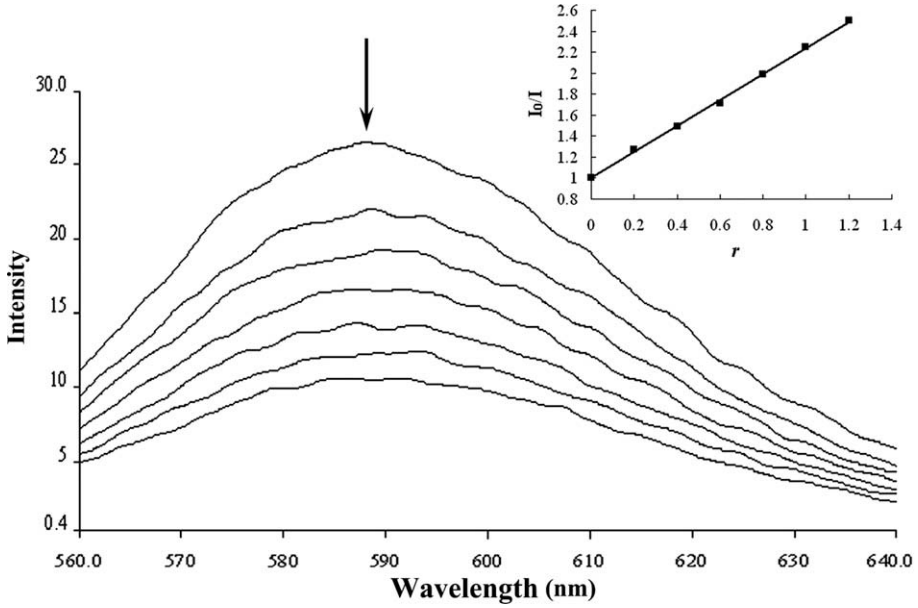

Figure 5. Fluorescene spectra of the binding of EB to DNA in 0.01 M Tris–HCl buffer at pH 7.2, in the absence and presence of increasing amounts of quercetin zinc(II) complex (from top to bottom, 0–120 μM), λ_{ex} = 500 nm, c_{EB} = 5 μM, c_{DNA} = 100 μM bp. The arrow shows the intensity decreased with increasing concentration of the complex. The inset is Stern–Volmer quenching plots of DNA–EB system by the complex. $r = c_{complex}/c_{DNA}$.

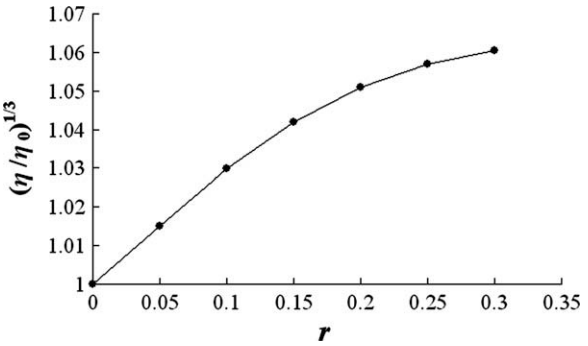

Figure 6. Effect of increasing amounts of quercetin zinc(II) complex on the relative viscosity of CT DNA in 0.01 M Tris–HCl buffer (pH 7.2) at 30 ± 0.1 °C. c_{DNA} = 50 μM, $r = c_{complex}/c_{DNA}$.

due to the complex interacts with DNA through intercalative binding, so releasing some free EB from DNA–EB complex,[25] which is consistent with the above absorption spectral results.

To investigate further the DNA-binding mode of $Zn(Que)_2(H_2O)_2$ complex, viscosity measurements on solutions of CT DNA incubated with the complex were performed. It is well known that intercalative DNA binding would cause elongation of DNA polymer by effecting separation of DNA base pairs, resulting in an increase in viscosity. In contrast, a partial or non-classical intercalation of the ligand could bend or kink DNA resulting in a decrease in its effective length with a concomitant decrease in its viscosity.[26,27]

The relative specific viscosity (η/η_0) of DNA generally reflects the increase in contour length associated with separation of DNA base pairs caused by intercalation. Figure 6 shows the increase in the relative specific viscosity of DNA when $Zn(Que)_2(H_2O)_2$ complex is added into CT DNA solution. So the results demonstrate that the complex could bind to DNA by intercalation mode, which is consistent with the above absorption and fluorescence spectral results.

2.2. Cytotoxicity study

The potential anti-proliferative effects of $Zn(Que)_2(H_2O)_2$ complex on the viability of tumor cell lines (HepG2, SMMC7721, and

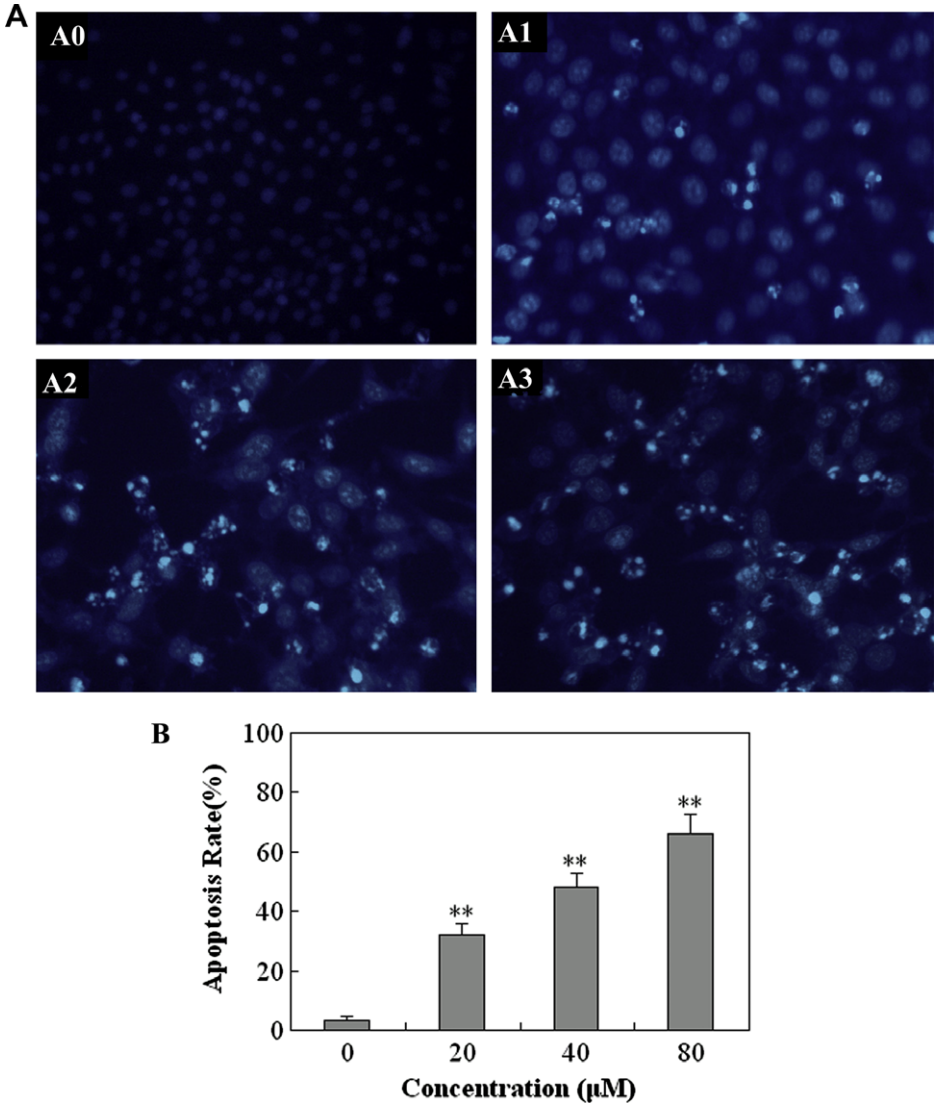

Figure 7. (A) The morphological changes of Hoechst33258-stained HepG2 cells after treatment with quercetin zinc(II) complex as observed under a fluorescent microscope (A0–A3). Cells were treated without the complex (A0) or with the complex at 20 μM (A1), 40 μM (A2) and 80 μM (A3) for 24 h. (B) Apoptotic cells were analyzed. Results are expressed as means ± SD (n = 3). $^{**}P < 0.01$ compared with control group.

A549) were detected by the MTT assay. The concentrations which showed 50% (IC_{50}) inhibition of the cell viability were analyzed by SPSS software and the results were listed in Table 1. From Table 1, the complex has a significant inhibition to growth and proliferation of all three tumor cells in a dose- and time-dependent manner. The cells showed different sensitivity to the compound with HepG2 cells appearing most sensitive among three cells lines. And the viability of HepG2, SMMC7721, and A549 cells was 9.2%, 17.6%, and 23.8%, respectively, after treatment with 100 μM of $Zn(Que)_2(H_2O)_2$ complex for 48 h. As shown in Table 1, the estimated IC_{50} values of the complex were 10.67, 14.10, and 21.03 μM obtained for 48h treatment of HepG2, SMMC7721, and A549 cells, respectively, but those of $(quercetin)_2$ were 33.69, 42.12, and 72.12 μM in the same conditions. The results illustrate that the cytotoxicity of $Zn(Que)_2(H_2O)_2$ complex is much higher than that of quercetin alone.

2.3. Apoptosis activity

To further address the death pattern, HepG2 cells were stained with Hoechst33258, after treatment with $Zn(Que)_2(H_2O)_2$ complex. The Hoechst33258 staining is sensitive to DNA and was used to assess changes in nuclear morphology. Results of Hoechst33258 staining assay showed that cells demonstrated apoptotic features such as nuclear shrinkage, chromatin condensation, or fragmentation, after treatment with the complex for 24 h. And the ratio of cells with a profile of chromatin condensation and fragmented fluorescent nuclei increased in a dose-dependent manner (Fig. 7A).

The apoptotic rate occurred in a dose-dependent manner calculated after Hoechst33258 staining assay, as shown in Figure 6B. After treatment with 80 μM of $Zn(Que)_2(H_2O)_2$ complex for 24 h, the apoptotic rate of HepG2 cells was more than 65%. These suggest that HepG2 cells undergo the typical morphologic changes of apoptosis after exposure to the complex.

2.4. Molecular modeling

The modeling results were tabulated in Table 2, which shows the change of total potential energies of the process of $Zn(Que)_2(H_2O)_2$ complex docking between DNA base pairs from major and minor groove. From the table, total potential energies of complex–DNA-binding system after intercalation, are much less than those of the system before intercalation, which may be associate with electrostatic interaction and space matching. Furthermore, total potential energy of complex–DNA-binding system formed by complex intercalating into C5G6 region from minor groove is less than those of other systems, illustrating that the minor groove binding of the complex in C5G6 region is the most preferential binding modeling of the interactions between the complex and DNA base pairs, which agrees with the above result of fluorescence measurement. Molecular modeling results, combined with cytotoxicity and apoptotic results as mentioned above, may suggest that the mechanisms of $Zn(Que)_2(H_2O)_2$ complex inducing tumor cell death and apoptosis may be similar to those of hedamycin, GC-rich sequence-selective DNA-binding antitumor agent,[28] which could preferentially intercalates into the GC-rich core promoter region of survivin, down-regulating surviving gene expression.

In addition, DNA cleavage of quercetin zinc(II) complex reported in our previous study[20] should be close related to DNA binding of the complex. Furthermore, some researches[29–31] demonstrated that the metal cations of metal complexes could coordinate with oxygen atom in the phosphodiester backbone of DNA, resulting in activation of P–O bond and promoting cleavage of DNA. On the basis of these researches, we proposed the model of DNA cleavage induced by $Zn(Que)_2(H_2O)_2$ as showed in Figure 8. Before cleaving DNA, the complex must be bound to DNA. The complex intercalating into DNA base pairs could promote the direct coordination between zinc cation and oxygen atom in the phosphodiester backbone of DNA, resulting in

Table 2
Total potential energies (kJ mol^{-1}) of intercalation of quercetin zinc(II) complex into DNA base pairs

Insert depth (Å)	Minor groove					Major groove				
	G3T4	T4C5	C5G6	G6A7	A7C8	G3T4	T4C5	C5G6	G6A7	A7C8
0	2626.36	2647.31	2639.39	2631.73	2655.65	2657.40	2641.29	2660.51	2643.43	2652.95
2	2566.28	2563.03	2552.41	2556.94	2599.76	2602.37	2583.44	2605.75	2578.30	2568.18
4	2534.53	2518.18	2512.19	2523.48	2562.86	2557.97	2564.70	2575.87	2544.04	2529.25
6	2508.17	2486.02	2466.15	2480.99	2533.94	2535.39	2551.35	2547.94	2508.90	2491.39
8	**2478.31**	2460.66	2440.55	2441.68	**2518.69**	2516.62	2536.79	2532.62	**2485.70**	**2473.01**
10	2492.40	**2434.15**	**2413.08**	**2439.21**	2533.81	**2496.58**	**2530.93**	**2521.88**	2497.46	2490.91

Bold value is the minimum value among each row of data.

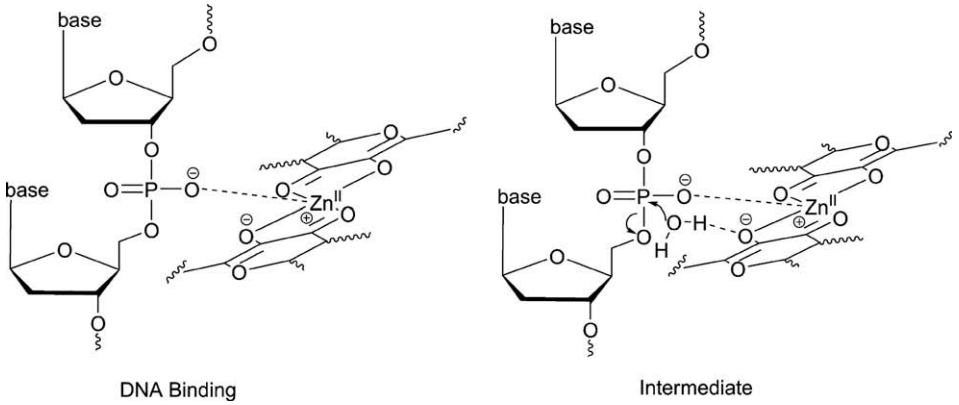

Figure 8. Proposed intermediate of DNA binding with quercetin zinc(II) complex.

activation of P–O bond. Furthermore, proximate hydroxyl oxygen atom, acting as Lewis base, pulls a proton from water molecule to promote its attack the phosphorus atom of the phosphodiester in the DNA backbone, which facilitates the formation of a pentacoordinated intermediate, as depicted in Figure 8. Finally, one of the P–O ester bonds of the phosphodiester in a DNA backbone is broken by the intramolecular charge delivery, resulting in the DNA cleavage. However, the real correlation of DNA binding and DNA cleavage needs to be confirmed through the further detailed research.

3. Conclusions

In the present study, the DNA-binding properties of $Zn(Que)_2(H_2O)_2$ complex have been examined by absorption spectroscopy, fluorescence spectroscopy, and viscosity measurements. Evidences are presented that $Zn(Que)_2(H_2O)_2$ complex could interact with DNA via intercalation mode. Furthermore, in the EB competition fluorescence assay, the Stern–Volmer quenching constant for this complex, K_{sq}, is obtained which is 1.24, illustrating that this complex could strongly bind to DNA as an intercalator competing with EB. In addition, on the basis of cytotoxicity assay, we find that $Zn(Que)_2(H_2O)_2$ complex has a significant inhibition to growth and proliferation of tumor cells (HepG2, SMMC7721, and A549) in a dose- and time-dependent manner, and that IC_{50} values of the complex are much less than that of quercetin alone. The results of Hoechst33258 staining suggest that the complex could induce apoptosis of tumor cells. Moreover, the results in molecular modeling show that the complex may be preferentially intercalate into C5G6 region of DNA helix from minor groove. Although the molecular modeling is not perfect, it is possible to point out that DNA-binding properties of quercetin zinc(II) complex are related to its cytotoxicity, and particularly that the complex may be intercalate into the GC-rich core promoter region of survivin, down-regulating surviving gene expression and promoting tumor cells apoptosis, like hedamycin.[28]

In summary, we have uncover the intercalation binding modes of $Zn(Que)_2(H_2O)_2$ complex with DNA involved in the cytotoxicity of the complex. The finding shows that DNA binding of the complex could play an important but not exclusive role in its antitumor activity. We are now conducting experiments on the in vivo test and studies of expression of protein related to apoptosis of the complex. In future, this complex, as an antitumor drug, might prove to be of application in target-based cancer therapy.

4. Experimental

4.1. Materials

All chemicals and reagents were purchased from commercial sources and were used without further purification. Quercetin, 3-(4,5-dimethylthiazol-2-yl)-2,5-diphenyl tetrazolium bromide (MTT), Hoechst33258, ethidium bromide (EB), calf thymus DNA (CT DNA), poly(dA)·poly(dT), and poly(dG)·poly(dC) were obtained from Sigma (Sigma Chemical Co., St. Louis, MO, USA). The Tris–HCl buffer solution was prepared with triple distilled water. The structure of quercetin zinc(II) complex, $Zn(Que)_2(H_2O)_2$, was reported in our previous study,[19] as shown in Figure 1. Each Zn(II) ion coordinates carbonyl oxygen, hydroxy oxygen atoms of quercetin and oxygen atoms of H_2O.

4.2. DNA-binding measurements

All the experiments involving the interaction of compound with CT DNA were conducted in Tris buffer (0.01 M Tris–HCl/50 mM NaCl, pH 7.2). The purity of the DNA was determined by monitoring the value A_{260}/A_{280} about 1.8–1.9:1, indicating that the DNA was sufficiently free of protein. The DNA concentration per nucleotide was determined by absorption spectroscopy using the molar absorption coefficient (6600 M^{-1} cm^{-1}) at 260 nm.

4.2.1. UV–vis spectra

UV–vis spectra were measured on a Lambda 900 UV/vis/NIR Spectrometer (Perkin–Elmer) in 0.01 M Tris buffer.[1,32] Spectroscopic titrations were carried out at room temperature to determine the binding affinity between DNA and $Zn(Que)_2(H_2O)_2$. Initially, the solutions (2000 μL) of the blank buffer and $Zn(Que)_2(H_2O)_2$ complex sample (10 μM) were placed in the reference and sample cuvettes (1 cm path length), respectively, and then first spectrum was recorded in the range of 250–460 nm. During the titration, aliquot (20 μL) of buffered DNA solution (concentration of 1 mM in base pairs) was added to each cuvette to eliminate the absorbance of DNA itself, and the solutions were mixed by repeated inversion. After the solutions were mixed for 10 min, the absorption spectra were recorded. The titration processes were repeated until there was no change in the spectra for four titrations at least, which indicated binding saturation had been achieved. The changes in the metal complex concentration were negligible due to dilution at the end of each titration.[32]

4.2.2. Fluorescence measurements

Fluorescence measurements[33] were made using Perkin–Elmer LS-50B fluorescence spectrophotometer with a slit width 5 nm for the excitation and emission beams. Fluorescence titrations were carried out by adding increasing amounts of CT DNA directly into the cell containing the solution of $Zn(Que)_2(H_2O)_2$ complex (c = 30 μM, 0.01 M Tris buffer, pH 7.2). To determine the selective binding of the complex to DNA with different sequences, another two kinds of DNA (poly(dA)·poly(dT) and poly(dG)·poly(dC)) were introduced to displace CT DNA.[22] The concentration range of the DNA was 0–60 μM bp. Emission spectra were recorded in the region 330–370 nm using an excitation wavelength of 312 nm. Fluorescence quenching study was conducted by adding increasing amounts of $Zn(Que)_2(H_2O)_2$ complex (0–120 μM) directly into the EB–DNA system (c_{EB} = 5 μM, c_{DNA} = 100 μM bp, 0.01 M Tris buffer, pH 7.2). And emission spectra were recorded in the region 520–650 nm using an excitation wavelength of 500 nm. All measurements were performed at 25 °C.

4.2.3. Viscosity measurements

Viscosity measurements were carried out using an Ubbelodhe viscometer maintained at a constant temperature at 30.0 ± 0.1 °C in a thermostatic bath.[32] Flow time was measured with a digital stopwatch and each sample was measured three times and an average flow time was calculated. Data are presented as $(\eta/\eta_0)^{1/3}$ versus binding ratio,[34] where η is the viscosity of DNA in the presence of the complex and η_0 is the viscosity of DNA in the absence of the complex. Viscosity values were calculated from the observed flow time of DNA-containing solutions ($t > 100$ s) corrected for the flow time of buffer alone (t_0), $\eta = t - t_0$.

4.3. Cell culture

Human hepatocellular liver carcinoma (HepG2), human hepatoma (SMMC7721), and human lung adenocarcinoma (A549) cell lines were obtained from the American Type Culture Collection (Rockville, MD, USA). The three cell lines were cultured in RPMI 1640 medium supplemented with 10% fetal bovine serum (FBS; HyClone, USA), 100 units/mL penicillin, 100 μg/mL streptomycin, L-glutamine (0.03%, w/v), and sodium bicarbonate (2.2%, w/v). Cell cultures were kept in a humidified incubator with 5% CO_2 at 37 °C.

And subcultures were performed with 0.05% trypsin–0.02% EDTA in phosphate-buffered saline (PBS; Gibco BRL Co., USA).

4.4. Cytotoxicity evaluation

The cytotoxicity or survival of cells in the presence or absence of the experimental agent was determined using a system based on MTT as described previously.[35] The tumor cells (HepG2, SMMC7721, and A549) were plated into 96-well microtiter plates at a density of 1×10^4 cells/well. After 24 h, culture medium was replaced by 200 μL RPMI 1640 medium supplemented with 10% fetal bovine serum in the presence of various concentration (0, 6.25, 12.5, 25, 50, and 100 μM) of $Zn(Que)_2(H_2O)_2$ complex or $(quercetin)_2$ (its concentration was calculated as two molecules), and the cells were incubated for 24, 48, and 72 h. The final concentration of solvent was less than 0.1% in cell culture medium. Culture solutions were removed and replaced by 90 μL culture medium. Ten microliters of sterile filtered MTT solution (5 mg/mL) in PBS (pH 7.4) was added to each well reaching a final concentration of 0.5 mg MTT/mL. Then cells were incubated at 37 °C for 4 h. After the medium and unreacted dye was removed, DMSO (200 μL) was added to each well. Absorbance at 490 nm of the dissolved solution was measured by a Bio-Rad 680 microplate reader (BIO-RAD, USA). The relative cell viability (%) related to control wells containing cell culture medium without tested compound was calculated by dividing the absorbance of treated cells by that of the control in each experiment. The IC_{50} which inhibits growth of 50% of cells relative to non-treated control cells was calculated as the concentration of tested compound by SPSS statistical software.

4.5. Apoptosis assessment by Hoechst33258 staining

Chromatin condensation was detected by nuclear staining with Hoechst33258. The HepG2 cells were cultured on coverslips, which were kept in a 60 Petri dish for 24 h before treatment. After treatment with 0, 40, 80 μM $Zn(Que)_2(H_2O)_2$ complex for 24 h, HepG2 cells were fixed with ice-cold methanol and acetic acid (3:1) at room temperature for 5 min and exposed to Hoechest33258 staining solution (5 μg/mL) at room temperature in the dark for 15 min. Samples were observed under a fluorescence microscope (Olympus BX-51, Japan).

4.6. Molecular modeling

Full geometry optimization of the complex starting at C_{2h} symmetry was carried out with the DFT method at the B3LYP/LanL2DZ level.[36] Molecular mechanics studies of DNA modeling were preformed using the INSIGHT II package. The structure of decameric DNA duplex 5′-d$(CCATTAATGG)_2$-3′ was built and optimized by molecular mechanics in force field of AMBER and ESFF. The processes of the complex intercalating into DNA were simulated by Docking method. The complex intercalated between base group pairs of DNA from the major groove and minor groove, respectively. Initially, the plane of the complex, over against the gap between DNA base pairs, was perpendicular to the axis of DNA helix. And the complex was placed at the outside of the DNA double helix, which was defined 0 as intercalation depth. Then geometry optimizations and the energy minimum calculation of the system of the complex intercalating into DNA base pairs were carried out. The complex move 2 Å into DNA base pairs, and geometry optimization and the energy minimum calculation are performed, which were repeated until the complex fully intercalated into DNA or energy of the system was 10 kJ mol^{-1} higher than that of the previous step. The interactions of DNA with the complex were examined by comparing the potential energy differences among different binding sites of both minor and major grooves.

Acknowledgments

This work was financially supported by the Natural Science Foundation Project of CQ CSTC (No. 2006BB1140), and the Natural Science Young Scholars Foundation of Chongqing University (No. 0221001104305).

References and notes

1. Song, Y.-M.; Wu, Q.; Yang, P.-J.; Luan, N.-N.; Wang, L.-F.; Liu, Y.-M. *J. Inorg. Biochem.* **2006**, *100*, 1685.
2. Kožurková, M.; Sabolová, D.; Janovec, L.; Mikeš, J.; Kovaľ, J.; Ungvarský, J.; Stefanisinová, M.; Fedorocko, P.; Kristian, P.; Imrich, J. *Bioorg. Med. Chem.* **2008**, *16*, 3976.
3. Tan, C.-P.; Liu, J.; Chen, L.-M.; Shi, S.; Ji, L.-N. *J. Inorg. Biochem.* **2008**, *102*, 1644.
4. Zuber, G.; Quada, J. C., Jr.; Hecht, S. M. *J. Am. Chem. Soc.* **1998**, *120*, 9368.
5. Hecht, S. M. *J. Nat. Prod.* **2000**, *63*, 158.
6. Metcalfe, C.; Thomas, J. A. *Chem. Soc. Rev.* **2003**, *32*, 215.
7. Silvestri, A.; Barone, G.; Ruisi, G.; Lo Giudice, M. T.; Tumminello, S. *J. Inorg. Biochem.* **2004**, *98*, 589.
8. Navarro, M.; Cisneros-Fajardo, E. J.; Sierralta, A.; Fernández-Mestre, M.; Silva, P.; Arrieche, D.; Marchán, E. *J. Biol. Inorg. Chem.* **2003**, *8*, 401.
9. Zhang, H.; Liu, C.-S.; Bu, X.-H.; Yang, M. *J. Inorg. Biochem.* **2005**, *99*, 1119.
10. Sheng, X.; Guo, X.; Lu, X.-M.; Lu, G.-Y.; Shao, Y.; Liu, F.; Xu, Q. *Bioconjugate Chem.* **2008**, *19*, 490.
11. Xu, H.; Zheng, K.-C.; Deng, H.; Lin, L.-J.; Zhang, Q.-L.; Ji, L.-N. *Dalton. Trans.* **2003**, *3*, 2260.
12. Xu, H.; Zheng, K.-C.; Deng, H.; Lin, L.-J.; Zhang, Q.-L.; Ji, L.-N. *New J. Chem.* **2003**, *27*, 1255.
13. Asadi, M.; Safaei, E.; Ranjbar, B.; Hasani, L. *New J. Chem.* **2004**, *28*, 1227.
14. Nègre-Salvayre, A.; Salvayre, R. *Free Radical Biol. Med.* **1992**, *12*, 101.
15. Afanasev, I. B.; Dorozhko, A. I.; Brodskii, A. V.; Kostyuk, V. A.; Potapovitch, A. I. *Biochem. Pharmacol.* **1989**, *38*, 1763.
16. Morel, I.; Lescout, G.; Cogrel, P.; Sergent, O.; Posdeloup, N.; Brissot, P.; Cillard, P.; Cillard, J. *Biochem. Pharmacol.* **1993**, *45*, 13.
17. Shao, H.-B.; Chu, L.-Y.; Lu, Z.-H.; Kang, C.-M. *Int. J. Biol. Sci.* **2008**, *4*, 8.
18. Rubens de Souza, F. V.; Wagner De Giovani, F. *Redox Repor* **2004**, *9*, 97.
19. Zhou, J.; Wang, L.-F.; Wang, J.-Y.; Tang, N. *Transition Met. Chem.* **2001**, *26*, 57.
20. Tan, J.; Wang, B.-C.; Zhu, L.-C. *Bioorg. Med. Chem. Lett.* **2007**, *17*, 1197.
21. Tan, J.; Wang, B.-C.; Zhu, L.-C. *Colloids Surf., B* **2007**, *55*, 149.
22. Li, W.-Y.; Zhu, S.-T.; He, X.-W. *Acta Chim. Sinica* **2002**, *60*, 105.
23. Lakowicz, J. R.; Weber, G. *Biochemistry* **1973**, *12*, 4161.
24. Liu, J.; Zhang, T.-X.; Lu, T.-B.; Qu, L.-H.; Zhou, H.; Zhang, Q.-L.; Ji, L.-N. *J. Inorg. Biochem.* **2002**, *91*, 269.
25. Boger, D. L.; Fink, B. E.; Brunette, S. R.; Tse, W. C.; Hedrick, M. P. *J. Am. Chem. Soc.* **2001**, *123*, 5878.
26. Satyanarayana, S.; Dabrowiak, J. C.; Chaires, J. B. *Biochemistry* **1992**, *31*, 9319.
27. Hirohama, T.; Kuranuki, Y.; Ebina, E.; Sugizaki, T.; Arii, H.; Chikira, M.; Selvi, P. T.; Palaniandavar, M. *J. Inorg. Biochem.* **2005**, *99*, 1205.
28. Wu, J.-G.; Ling, X.; Pan, D.-L.; Apontes, P.; Song, L.; Liang, P.; Altieri, D. C.; Beerman, T.; Li, F.-Z. *J. Biol. Chem.* **2005**, *280*, 9745.
29. Huo, F.-J.; Yin, C.-X.; Yang, P. *Bioorg. Med. Chem. Lett.* **2007**, *17*, 932.
30. An, Y.; Liu, S.-D.; Deng, S.-Y.; Ji, L.-N.; Mao, Z.-W. *J. Inorg. Biochem.* **2006**, *100*, 1586.
31. Rossi, L. M.; Neves, A.; Hörner, R.; Terenzi, H.; Szpoganicz, B.; Sugai, J. *Inorg. Chim. Acta* **2002**, *337*, 366.
32. Rajendiran, V.; Murali, M.; Suresh, E.; Palaniandavar, M.; Periasamy, V. S.; Akbarsha, M. A. *Dalton Trans.* **2008**, *8*, 2157.
33. Tan, J.-H.; Lu, Y.-J.; Huang, Z.-S.; Gu, L.-Q.; Wu, J.-Y. *Eur. J. Med. Chem.* **2007**, *42*, 1169.
34. Cohen, G.; Eisenberg, H. *Biopolymers* **1969**, *8*, 45.
35. Mosmann, T. *J. Immunol. Methods* **1983**, *65*, 55.
36. Foresman, J. B.; Frisch, A. E. *Exploring Chemistry with Electronic Structure Methods*, 2nd ed.; Gaussian: Pittsburgh, PA, 1996.